

Characteristics of pulsatile flow with the reverse flow in the grooved channel

Junxiu PAN^{*1}, Yongning BIAN^{*1}, Hirofumi ARIMA^{*2} and Yasuyuki IKEGAMI^{*2}

^{*1}State Key Laboratory of Structural Analysis for Industrial Equipment
Dalian University of Technology, 116024, China

^{*2}Institute of Ocean Energy, Saga University, 840-8502, Japan

Abstract

The characteristics of pulsatile flow with the reverse flow in the grooved channel are investigated experimentally. Three flow parameters are considered: the net flow Reynolds number, the oscillatory fraction of the flow rate and the oscillatory frequency. The flow structures are visualized using the aluminum dust method. It is observed that the flow tends to be more unstable in the deceleration phase for the pulsatile flow. Meanwhile, the experimental oscillatory fraction of the flow rate is easier to reach the theoretical value at lower oscillatory frequency. Furthermore, it is found that the oscillatory fraction of the local pressure decreases with the increase of the period of oscillation, and the oscillatory fraction of the downstream local pressure is larger than that of the upstream local pressure.

Keywords: pulsatile flow, grooved channel, flow visualization, oscillatory fraction

1. Introduction

Ocean thermal energy conversion (OTEC) is a system which takes advantages of the temperature difference between the warm water at the surface of the ocean and cold water of the depths. However, the typical thermal efficiency of the Rankine cycle is only 3–5% which is primarily limited by the finite temperature difference (Khan et al., 2017). The authors and other researchers made researches about how to improve the thermal efficiency of the OTEC system (Bian et al., 2019). It was found that both double flute tube-type and plate-type heat exchangers are best fitted for the OTEC (Uehara et al., 1984).

In recent years, the characteristics of heat transfer in grooved channels have attracted many researchers' attention. Nishimura et al. (2004) studied mass-transfer enhancement and fluid dynamic behavior in a wavy-walled tube for pulsatile flow. They concluded that the unstable flow leads to remarkable fluid mixing and contributes to the mass-transfer enhancement. Bian et al. (2009) studied the relationship between the transitional characteristic and the enhancement mechanism in an axisymmetric wavy-walled tube under steady flow. They pointed that the most effective mass transfer enhancement occurred just before the transition flow regime. Zhang et al. (2018) experimentally analyzed the oscillatory flow in the grooved channel. They proposed that there is some difference between the experimental oscillatory fraction and the theoretical oscillatory fraction, and the experimental oscillatory fraction is close to the theoretical value with a lower Reynolds number. Huang et al. (2017) carried out the experimental study in the relationship between the characteristics of the pressure drop and the laminar pulsatile flow. They found that the overall pressure drop decreases with increase of the oscillatory frequency. Sun et al. (2010) studied the self-sustained flow in grooved channels. They found that the internal pressure of the channels strongly affects the amplitude of the self-sustained wave and increasing the pressure of the channels makes the amplitude higher.

Received date 2019.7.1

Email of the corresponding author: ybian@dlut.edu.cn

The present study deals with the characteristics of the pulsatile flow in the grooved channel. The effects of oscillatory frequency and Reynolds number on the experimental oscillatory fraction and the oscillatory fraction of the overall pressure drop and the local pressure are examined.

2. Experimental system

The diagram of the experimental system is shown in Fig. 1 and all the experimental apparatus are consistent with the previous ones. The city water is used as the working fluid and the net flow is provided by a centrifugal pump. The volumetric flow rate of the pulsatile is given as:

$$Q_i = Q_s + Q_0 \sin(2\pi ft) \quad (1)$$

where Q_s is the net flow rate which is determined with a flow-meter, f is the frequency of the pulsatile flow, t is the flow time, Q_0 is the amplitude of the pulsatile flow and it is expressed as:

$$Q_0 = 2\pi fs(\pi D_p^2/4) \quad (2)$$

where, $D_p = 50\text{mm}$ is the diameter of the piston.

The test section is depicted in Fig. 2. The grooved channels consist 55 grooved modules and the length of every grooved module is $L = 20\text{mm}$, $l = 10\text{mm}$, $W = 200\text{mm}$, $h = 2.5\text{mm}$. The local pressures $P_n(n=1,2,3\dots 8)$ are measured at different locations which are shown in Fig. 3.

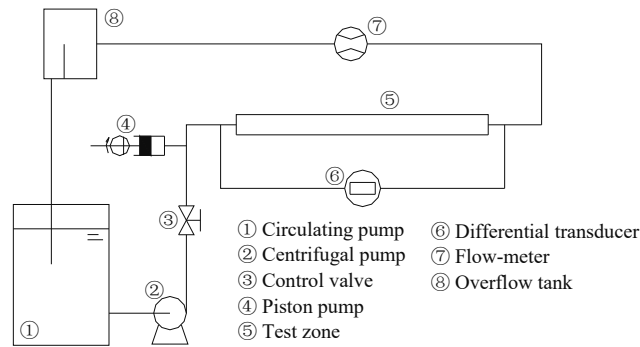


Fig. 1 Diagram of the experimental system

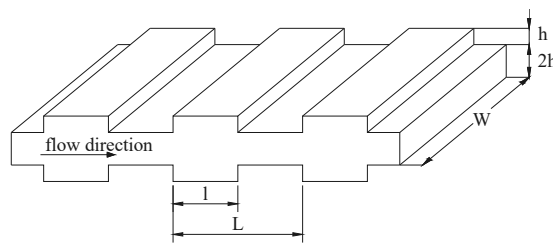


Fig. 2 Dimensions of the grooved channels

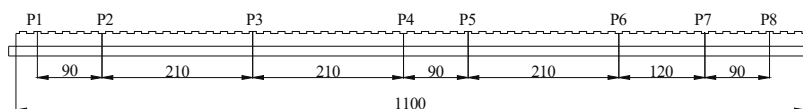


Fig. 3 Locations of the local pressure measurement

To get a better understanding of the pulsatile flow, some parameters are defined as follows:

The net flow Reynolds number (Re)

$$Re = \rho u h / \mu \quad (3)$$

where ρ and μ are the density and the viscosity of water respectively. The characteristic velocity of the flow u is calculated by:

$$u = 3/2 * u_s \quad (4)$$

where u_s is calculated as follow

$$u_s = Q_s / (2Wh) \quad (5)$$

The oscillatory fraction (P) of the flow rate

$$P = Q_0 / Q_s \quad (6)$$

The oscillatory fraction of the overall pressure drop (P')

$$P' = (\Delta P_{max} - \Delta \bar{P}) / \Delta \bar{P} \quad (7)$$

where ΔP_{max} is the instantaneous max value of the overall pressure drop, $\Delta \bar{P}$ is the time-averaged pressure drop.

The oscillatory fraction of the local pressure (P'_i)

$$P'_i = (P_i - \bar{P}_i) / \bar{P}_i \quad (8)$$

where P_i ($i=3,5,7$) is the instantaneous value of the local pressure, \bar{P}_i is the time-averaged value of the local pressure.

The instantaneous velocity u_i is depicted as:

$$u_i = u_s + P * u_s * \sin(2\pi f t) \quad (9)$$

The aluminum dust method is used to visualize the flow patterns. The aluminum dust method, i.e. perfusion with a suspension of aluminum particles which are about 40 μm in diameter, enables us to observe the pathlines approximately corresponding to streamlines in the whole flow field. Besides, the flow patterns are recorded by a digital video camera. All the experiments are conducted at the room temperature.

3. Results and discussion

3.1 Filter processing

In order to reduce the interference of noise in the experiment, the experimental data, i.e. the signal of the volume flow rate and the pressure drop, need to be filtered. As can be seen in Fig. 4, all the experimental data are processed 1Hz low pass fit filter. Though there is a slight deviation between the experimental data and the filtered data at the beginning and end of the experiment, the filtered data in the middle section are consistent with the experimental data. Therefore the following discussions are based on the filtered data in the middle section.

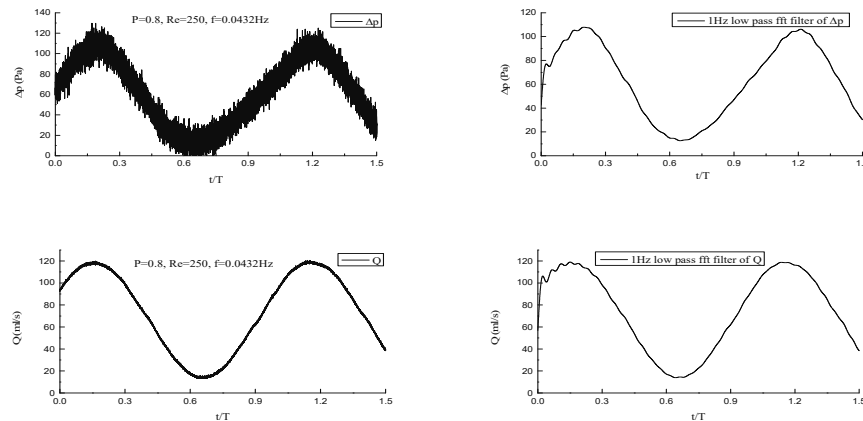


Fig. 4 Comparison of the experimental data with the filtered data.

3.2 Experimental flow patterns

4 kinds of flow patterns during one oscillation cycle for $P=1.6$ $Re=250$ and $f=0.0721$ deserves attention. As is shown in Fig. 5, when $t/T=0$, two stable symmetric vortexes form in the grooved area and the pathlines of the main flow are parallel to each other. It belongs to “stable” state and marked as “+”. It is easy to notice that when $t/T=0.25$, i.e. the instantaneous flow reaches a peak value, the particle pathlines are highly disturbed and the main flow becomes unstable. It indicates the turbulent motion and marked as “-”. It is apparent that when $t/T=0.625$ and $t/T=0.875$, the grooved area is filled with two large vortexes, and locations of all particles are almost motionless. Phenomenon like these implies the flow almost stops (i.e. the flow rate is close to 0) and marked as “s”. Besides when $t/T=0.75$, the fluid mixing area of the grooved region and the mainstream region appears at the upstream of the groove. It suggests there exists a reverse flow and marked as “r”. Moreover, it is interesting to observe that the particle pathlines at $t/T=0.375$ are more unstable than that at $t/T=0.125$ although their flow rates are the same. The same phenomenon can be seen when $t/T=0$ and $t/T=0.5$, therefore the flow tends to be more unstable in the deceleration phase. Which has been validated in Nishimura et al. (2004). Furthermore, based on Eq. (9) the flow rate is 0 only when $t/T=0.607$ and $t/T=0.893$, and the flow should be a reverse flow when $t/T=0.625$ and $t/T=0.875$. However, the actual behavior shows obviously different results with the theoretical value. Besides the errors from experimental photographing, it is deduced that the experimental oscillatory fraction (P) of the flow rate is lower than the theoretical value (P_0) based on Eq. (9).

3.3 Difference between P and P_0 .

To investigate whether the experimental oscillatory fraction of the flow rate (P) reaches the theoretical value (P_0), the experimental oscillatory fractions of the flow rate at different working conditions have been calculated and plotted in Fig. 6 and Fig. 7. Figure 6 shows the relationship between P and the periods of oscillation (T) at different P_0 and $Re=375$. It is not difficult to notice that P increases with T . Which means P is easier to reach P_0 at lower f . Furthermore, P is easier to reach P_0 when P_0 is set lower.

Figure 7 illustrates the relationship between P and the pulsation strokes (s) at different Re and $P_0=1.6$. It is noted that P increases with s , which also means P is easier to reach P_0 at lower f based on Eq. (2). Besides, P decreases with the increase of Reynolds number. Which means P is easier to reach P_0 at lower Reynolds number.

3.4 The effect of the T on P' and P'_i .

Figure 8 describes the effect of T on P' under different theoretical oscillatory fractions of the flow rate (P_0). P' increases with the increase of T , and it rises with the increase of P_0 . It is almost identical to P . It suggests the flow tends to be more unstable at lower f .

Figure 9 describes the effect of T on P'_i under different P_0 . It is seen that P'_i decreases with the increase of T . Moreover, it is interesting to note that the oscillatory fraction of the downstream local pressure is larger than that of the upstream local pressure. It indicates that downstream flow is more unstable than upstream flow. In addition, P'_i rises as P_0 increases.

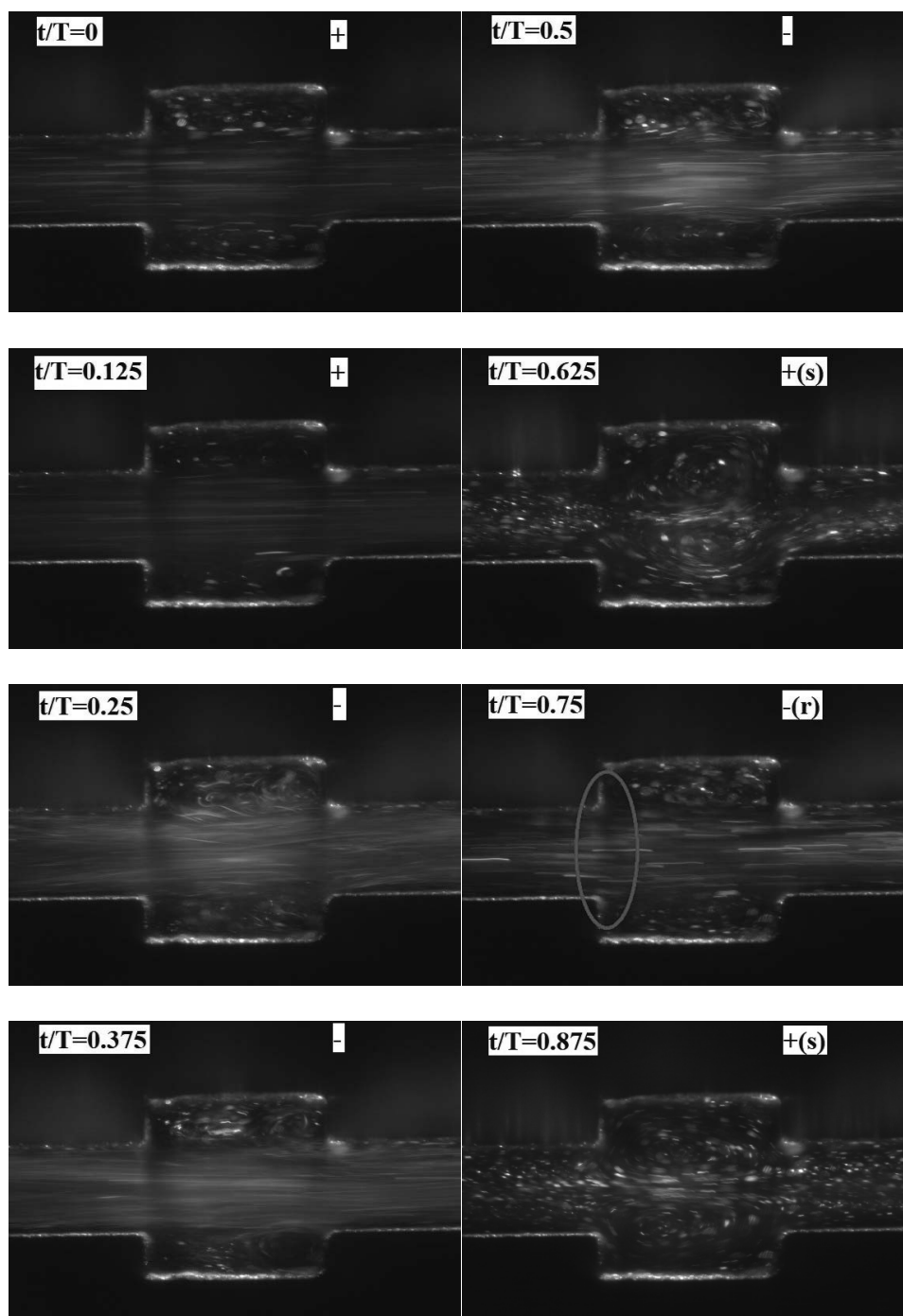


Fig. 5 Experimental flow patterns for $P=1.6$ $Re=250$ and $f=0.0721$.

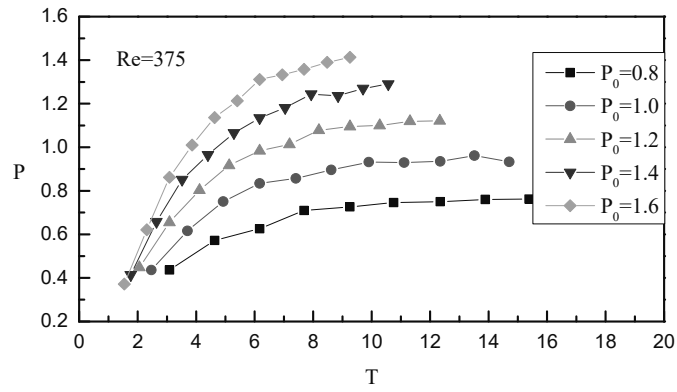


Fig. 6 Relationship between P and T at different P_0 and $Re=375$.

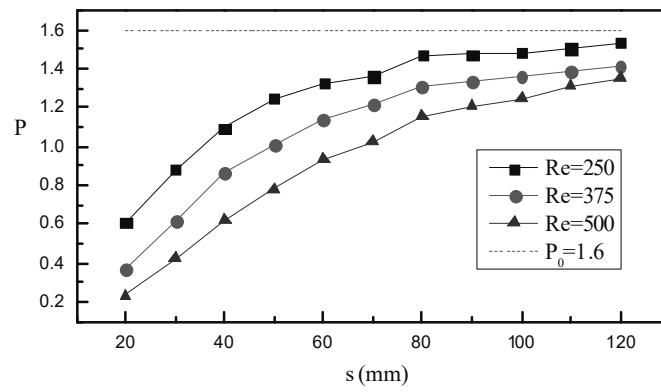


Fig. 7 Relationship between P and s at different Re and $P_0=1.6$.

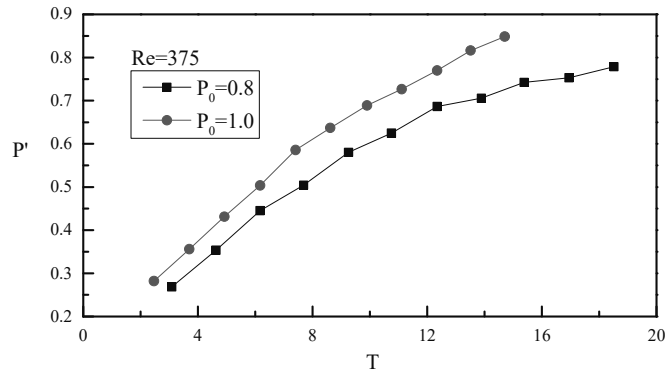


Fig. 8 Effect of T on P' under different P_0 .

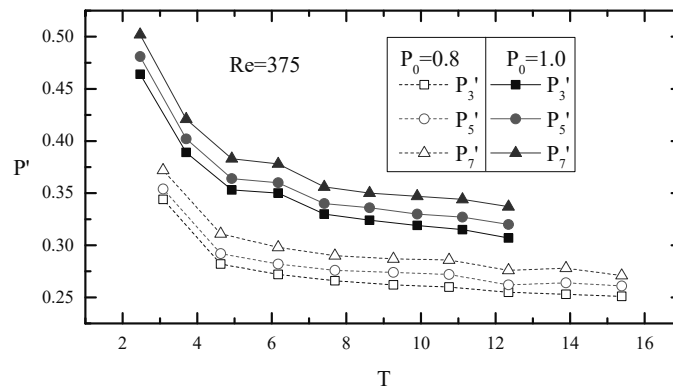


Fig. 9 Effect of T on P_i' under different P_0 .

4. Conclusions

In this paper, the characteristics of the pulsatile flow in the grooved channel are explored experimentally. The main conclusions are obtained as follows:

- (1) For the pulsatile flow, the flow tends to be more unstable in the deceleration phase.
- (2) P is easier to reach P_0 at lower f , lower P_0 or lower Reynolds number.
- (3) P' increases with the increase of T , and it rises with the increase of P_0 .
- (4) P_i' decreases with the increase of T , and the oscillatory fraction of the downstream local pressure is larger than that of the upstream local pressure.

The above results can be used as a useful reference for the design and operation of high efficiency heat exchangers.

Acknowledgment

This study is sponsored by the cooperative Research Program of IOES(No. 18A07).

References:

- Khan, N., Kalair, A., Abas, N., & Haider, A., Review of ocean tidal, wave and thermal energy technologies, *Renewable and Sustainable Energy Reviews*, Vol.72, (2017), pp. 590-604.
- Bian, Y., Pan, J., Liu, Y., Zhang, F., Yang, Y., & Arima, H., Performance analysis of a combined power and refrigeration cycle, *Energy Conversion and Management*, Vol.185, (2019), pp. 259-270.
- Uehara, H., Kusuda, H., Monde, M., Nakaoka, T., & Sumitomo, H., Shell-and-plate-type heat exchangers for OTEC plants, *Journal of solar energy engineering*, Vol.106, No.3 (1984), pp. 286-290.
- Nishimura, T., Bian, Y. N., & Kunitsugu, K., Mass - transfer enhancement in a wavy - walled tube by imposed fluid oscillation, *AIChE journal*, Vol.50, No.4 (2004), pp. 762-770.
- Bian, Y., & Jia, B., Mass transfer characteristics in an axisymmetric wavy-walled tube for pulsatile flow with backward flow, *Heat and mass transfer*, Vol.45, No. 6 (2009), pp. 693-702.
- Zhang, F., Bian, Y., Arima, H., & Ikegami, Y., Difference between Experimental and Theoretical Pulsatile Flow in Grooved Channel, *OTEC*, Vol.23, (2018), pp. 1-6.
- Huang, H., ARIMA, H., BIAN, Y., & IKEGAMI, Y., Pressure Drop Characteristics of Laminar Pulsatile Flow in Grooved Channel with Different Groove Lengths, *OTEC*, Vol.22, (2017), pp. 1-6.
- Sun, F., Bian, Y., Arima, H., Ikegami, Y., & Xu, X., Strength characteristics of the self-sustained wave in grooved channels with different groove length, *Heat and mass transfer*, Vol.46, No.11, (2010), pp. 1229-1237.